ELSEVIER

Journal of Alloys and Compounds 311 (2000) 124–129

Journal of ALLOYS AND COMPOUNDS

www.elsevier.com/locate/jallcom

X-ray diffraction and magnetic properties of β-$Mn_{1-x}Os_x$ alloys

R. Yamauchi*, M. Miyakawa, K. Sasao, K. Fukamichi

Department of Materials Science, Tohoku University, Aoba-yama 02, Aoba-ku, Sendai 980-8579, Japan

Received 10 March 2000; accepted 16 June 2000

Abstract

The X-ray powder diffraction patterns of $Mn_{1-x}Os_x$ ($x \leqq 0.36$) alloys quenched from 1223 K show the β-Mn structure in which Os atoms preferentially occupy site 1, whereas the patterns of the specimens quenched from 873 K exhibit the α-Mn structure below $x = 0.14$. Using the resultant data, we have determined the phase diagram of the Mn–Os alloy system for the first time. The Néel temperature of β-$Mn_{1-x}Os_x$ ($x \leqq 0.36$) alloys determined from the magnetic susceptibility increases with increasing Os concentration. The electronic specific heat coefficient, γ, of samples with relatively low Os concentration is considerably large due to spin fluctuations.

Keywords: β-MnOs alloy; Phase diagram; Néel temperature; Specific heat; Spin fluctuation

1. Introduction

Pure Mn metal is known to have four phases, α, β, γ and δ, as the temperature increases. α-Mn has a complex cubic structure with 58 atoms per unit cell and four kinds of crystallographical sites [1,2], and exhibits an antiferromagnetic ordering below 95 K [3]. The δ and γ phases adopt a body-centered and a face-centered cubic structure, respectively, and these two phases are hardly stabilized at room temperature. For the δ-Mn phase, there is little experimental information on the magnetic properties. The γ-Mn phase is stabilized by elements such as Fe, Pd and Pt at room temperature when quenching from high temperatures, and these γ-Mn alloys are antiferromagnetic with a relatively high Néel temperature [4–6]. Recently, γ-Mn alloys have been studied extensively as a pinning layer of spin-valves which control the GMR (giant magnetoresistance) effect [7–9]. We have investigated the fundamental magnetic properties of γ-MnRh alloys and pointed out that the difference in the Néel temperature, depending on the substitutional elements for γ-Mn alloys, is associated with the number of 3d electrons in the Mn site [10,11]. In other words, theoretical calculations predict that the antiferromagnetic exchange interaction of γ-Mn becomes stronger with decreasing 3d electron number at the Mn site. Therefore, it is expected that γ-MnRu and γ-MnOs alloys will exhibit a higher Néel temperature than γ-MnRh [12] and γ-MnIr alloys [13] reported to have a very high Néel temperature.

The β-Mn phase can easily be obtained by quenching, and its crystal structure is cubic with two kinds of crystallographic sites consisting of 20 atoms per unit cell [14]. Pure β-Mn metal shows no magnetic ordering down to low temperatures, and it is regarded as an enhanced Pauli paramagnet from the experimental data of magnetic susceptibility [15], low-temperature specific heat [16] and NMR [17]. The absence of magnetic ordering down to low temperatures is explainable in terms of the frustration due to the peculiar geometry of the crystal structure [18,19]. On the other hand, it has been reported that alloying induces magnetic ordering [20–24], and β-MnFe, -MnCo and -MnNi alloys are regarded as weak antiferromagnets within the framework of SCR (self-consistent renormalization) theory [25].

For the Mn–Os system, the concentration dependence of the Néel temperature of α-$Mn_{1-x}Os_x$ alloys has been reported. However, the concentration region is restricted to below $x = 0.01$ [26]. No phase diagrams have so far been established and there is little information on the magnetic properties of Mn–Os alloys and compounds. In the present study, the phase diagram below $x = 0.36$ has been obtained from X-ray powder diffraction and DSC (differential scanning calorimetry) measurements. The γ-MnRu phase has been obtained by quenching [27] and, as expected, the Néel temperature is higher than that of γ-MnIr [13] and

*Corresponding author.

E-mail address: rie@maglab.material.tohoku.ac.jp (R. Yamauchi).

0925-8388/00/$ – see front matter
PII: S0925-8388(00)01090-2

γ-MnRh alloys [12] in the disordered state. Unfortunately, no γ-MnOs phase is obtainable by quenching. The concentration dependence of the lattice constant and the Néel temperature of β-$Mn_{1-x}Os_x$ has been investigated. Furthermore, the electronic specific heat coefficient has been discussed in terms of spin fluctuations.

2. Experimental

The starting materials were 99.985% pure electrolytic Mn flakes and 99.9% pure Os powder. Before alloying, surface oxidation of the Mn flakes was removed by etching with very dilute nitric acid, and they were arc-melted in order to release gas in the Mn flakes. The Os powders were also arc-melted in order to make Os ingots. The specimens were prepared by arc-melting in an argon gas atmosphere purified with a Ti getter, and turned over and remelted four times to homogenize. α-Mn is stable at room temperature, and the phase transition to β-Mn occurs at approximately 1000 K [28]. Therefore, the β-$Mn_{1-x}Os_x$ phase is also obtainable by rapid quenching from high temperatures. For homogenization, annealing was carried out in an evacuated quartz tube at 1223 K for 30 min. For the investigation of phase stability, samples annealed for 7 days at 873 or 673 K were quenched in ice water. The concentration of the samples was determined by EDXS (energy dispersive X-ray spectroscopy). The crystal structure and the room temperature lattice constant were obtained by X-ray powder diffraction with Cu Kα radiation. The structural phase transition temperature was clarified by DSC measurements. The temperature dependence of the magnetic susceptibility was measured with a SQUID magnetometer from 4.2 to 300 K in a magnetic field of 1 T. The low-temperature specific heat measurement was performed by a relaxation method to determine the relation between the electronic specific heat coefficient and the spin fluctuations.

3. Results and discussion

Fig. 1 shows the room temperature X-ray powder diffraction patterns of $Mn_{1-x}Os_x$ ($x = 0.06$, 0.13, 0.15, 0.20, 0.33 and 0.36) alloys quenched from 1223 K. The calculated diffraction intensities of pure β-Mn metal (space group $P4_132$; lattice constant $a = 0.6315$ nm) and those of two kinds of β-$Mn_{0.6}Os_{0.4}$ alloys are also shown, respectively, below and above in the same figure for comparison. The crystal structure of the β-Mn phase is illustrated in Fig. 2. The Mn atoms at site 2 form corner sharing triangles lying in the (111) plane. Although the β-$Mn_{0.6}Os_{0.4}$ alloy was not prepared, this composition was selected for easy calculation. In the calculations for the β-$Mn_{0.6}Os_{0.4}$ alloys it was assumed that all the Os atoms occupy site 1 (a) or site 2 (b) in the β-Mn lattice with $a = 0.6550$ nm, the latter being extrapolated from the concentration dependence of the lattice constant in Fig. 3. As can be seen, the peak shift to lower angles indicates lattice expansion with increasing Os concentration. Moreover, the experimental intensities of the β-$Mn_{1-x}Os_x$ alloys gradually change from the intensities of pure β-Mn metal to those of (a) for the β-$Mn_{0.6}Os_{0.4}$ alloy. For example, the intensities of the 110 and 111 peaks increase, whereas the intensity of the 210 peak decreases with

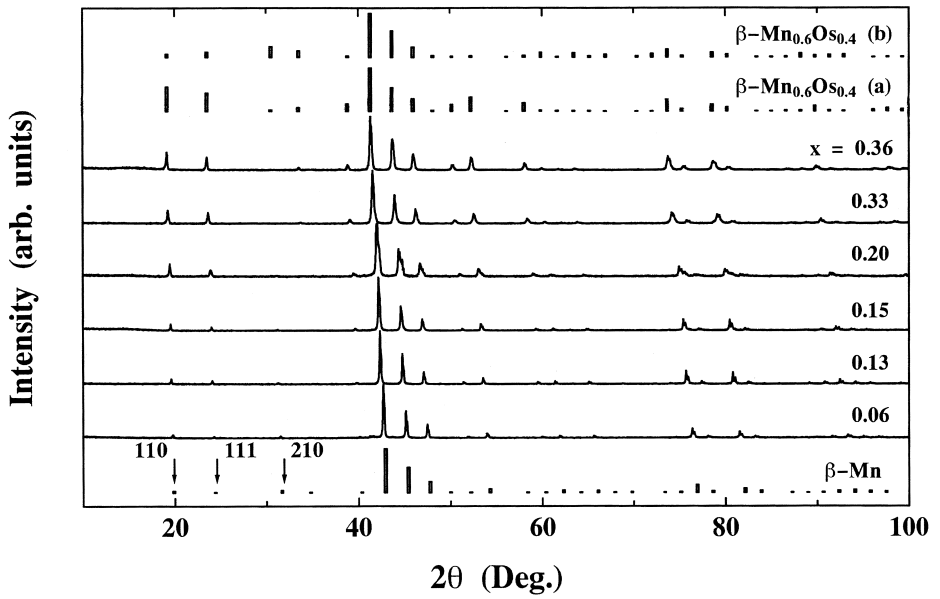

Fig. 1. Room temperature X-ray powder diffraction patterns of $Mn_{1-x}Os_x$ ($x = 0.06$, 0.13, 0.15, 0.20, 0.33 and 0.36) alloys quenched from 1223 K. The calculated diffraction intensities of pure β-Mn metal and β-$Mn_{0.6}Os_{0.4}$ alloys are given for comparison. The two kinds of calculations for β-$Mn_{0.6}Os_{0.4}$ alloy were made by assuming that all Os atoms occupy site 1 (a) or site 2 (b).

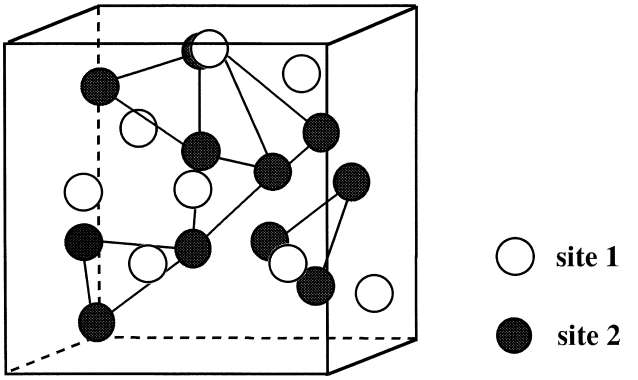

Fig. 2. Crystal structure of the β-Mn phase. Mn atoms at site 1 (○) and site 2 (●). Note that the Mn atoms at site 2 construct the corner sharing triangles lying in the (111) plane.

increasing Os concentration. These clear changes originate from the large difference between the atomic scattering factor of Mn and Os atoms. We can conclude that the Os atoms preferentially occupy site 1 by comparing the calculated intensities between (a) and (b) for the β-$Mn_{0.6}Os_{0.4}$ alloy in Fig. 1. The Os concentration dependence of the room temperature lattice constant of β-$Mn_{1-x}Os_x$ ($x \leqq 0.36$) alloys quenched from 1123 K is shown in Fig. 3. As mentioned above, the lattice constant increases with increasing Os concentration.

Fig. 4 shows the room temperature X-ray powder diffraction patterns of $Mn_{1-x}Os_x$ ($x = 0.13$, 0.20 and 0.33) alloys quenched from 873 K. In the same figure, the calculated diffraction intensities of α-Mn (space group $I\underline{4}3m$; lattice constant $a = 0.8912$ nm) and β-$Mn_{0.6}Os_{0.4}$, in which all Os atoms are assumed to occupy site 1 in the β-Mn lattice, are shown below and above, respectively. The diffraction patterns of the samples with $x = 0.13$ and $x = 0.33$ show a single phase of the α-Mn and β-Mn structures, respectively. However, the diffraction patterns

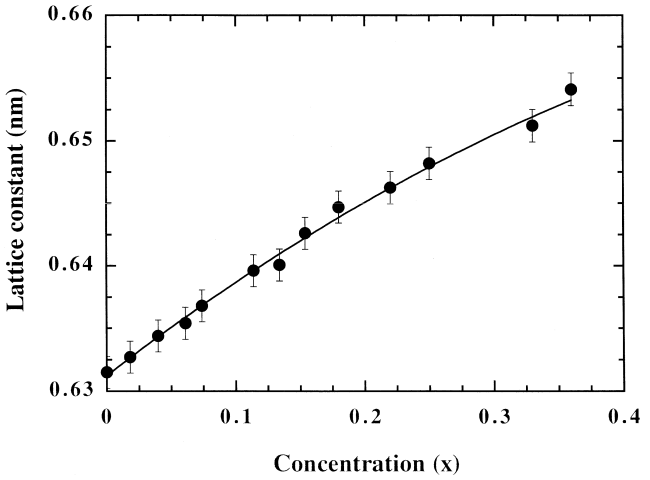

Fig. 3. Concentration dependence of the room temperature lattice constant of β-$Mn_{1-x}Os_x$ alloys quenched from 1223 K.

of the sample with $x = 0.20$ show a mixed phase of the α and β phases. It is well known that pure Mn transforms from the α to the β phase at about 1000 K [28]. Therefore, using the X-ray diffraction data for the samples quenched from 1223, 873 and 673 K, and the DSC data, we can obtain the phase diagram for the Mn–Os system, as given in Fig. 5. In the DSC measurements, an anomaly is clear because of the structural phase transition from the α to β phase. The solid circles in the figure indicate the transition temperatures derived from DSC measurements. However, the anomaly in the DSC curves due to the phase separation from the α to the mixed α and β phase is not so clear. Although the γ-MnOs phase may exist in the higher temperature region, we cannot obtain it under the present heat-treatment conditions. Theoretically, the Néel temperature of the γ-Mn phase increases as the 3d electron number in the Mn site decreases [10,11]. However, it is worth noting that the γ-phase is easily obtained by quenching and annealing in the Mn–Ir [13,29] and Mn–Rh [12,29] alloy systems, and by quenching in the Mn–Ru alloy system [27]. Eventually, the γ-phase is no longer obtainable by quenching in the present Mn–Os alloy system. That is to say, the γ-Mn phase becomes more unstable with decreasing 3d electron number.

Fig. 6 shows the temperature dependence of the magnetic susceptibility of the β-$Mn_{1-x}Os_x$ ($x = 0.06$, 0.13, 0.20, 0.33 and 0.36) alloys quenched from 1123 K. It has been reported that pure β-Mn metal is an enhanced Pauli paramagnet with an antiferromagnetic correlation [15] and that β-Mn alloys become weakly antiferromagnetic [20–24]. Therefore, the small peak and the inflection point in the magnetic susceptibility curves are defined as the Néel temperature T_N. The concentration dependence of the Néel temperature of β-$Mn_{1-x}Os_x$ alloys is shown in Fig. 7. The Néel temperature increases with increasing Os concentration and a steeper increase takes place above about 13% Os. The occupation site of the substitutional atom is very important for the magnetic properties of β-Mn alloys, because the magnetic properties of Mn atoms are quite different, depending on site 1 and site 2. NMR studies demonstrate that the value of the nuclear spin-lattice relaxation rate at site 2 is about 20 times larger than that at site 1 [17,30], indicating that the electronic state of Mn at the former site is more magnetic than that at the latter site. For β-MnAl alloys in which Al atoms occupy site 2, it has been reported from the results of NMR and magnetic measurements that its ground state is a spin-glass-like state [31,32]. The magnetic susceptibility of β-$Mn_{1-x}Al_x$ alloys with $x = 0.30$ shows a field-cooling effect at low temperatures and obeys a modified Curie–Weiss law above the spin freezing temperature [31]. Although we performed a field-cooling magnetic measurement for the β-$Mn_{0.87}Os_{0.13}$ alloy, no field-cooling effect was observed and its paramagnetic susceptibility gradually increases in analogy with an itinerant-type $(CoMn)_{1-x}Fe_x$ antiferromagnet [33,34].

Fig. 8 shows the low-temperature specific heat C for

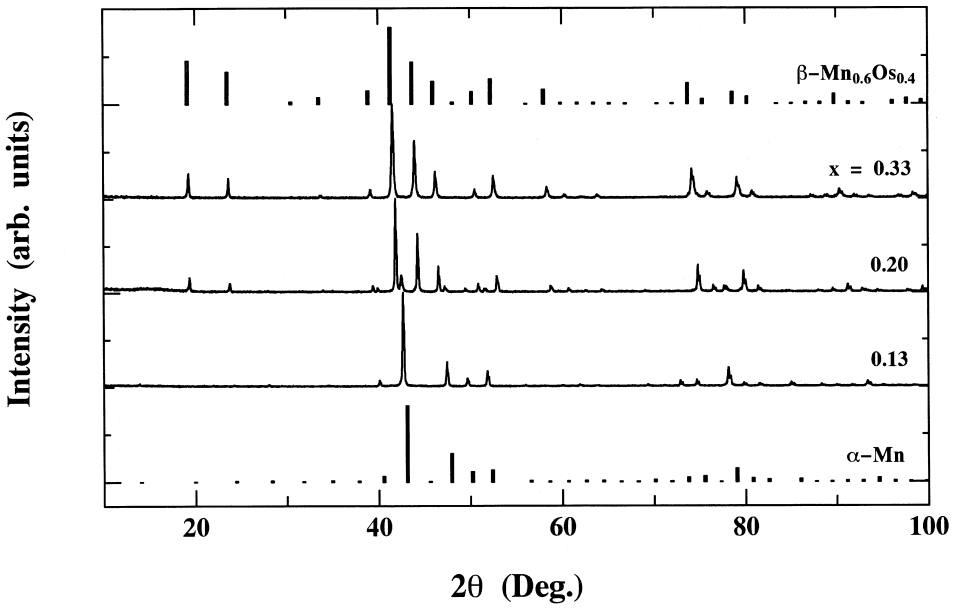

Fig. 4. Room temperature X-ray powder diffraction patterns of $Mn_{1-x}Os_x$ ($x = 0.13$, 0.20 and 0.33) alloys quenched from 873 K, together with the calculated diffraction intensities of pure α-Mn metal and β-$Mn_{0.6}Os_{0.4}$ alloy.

β-$Mn_{1-x}Os_x$ alloys with $x = 0.06$, 0.15 and 0.20, in which C/T is plotted against T^2. For all samples, C/T is proportional to T^2 and the electronic specific heat coefficient γ was estimated by linear extrapolation. The values of γ for the samples with $x = 0.06$, 0.13 and 0.20 are about 44, 25 and 14 mJ mol^{-1} K^{-2}, respectively. It is clear that the γ value of the β-MnOs alloys is enhanced, compared with the band term of about 8 mJ mol^{-1} K^{-2} for pure β-Mn metal [35]. In fact, it has been reported that the γ value for pure β-Mn metal regarded as an enhanced Pauli paramagnet is estimated to be about 70 mJ mol^{-1} K^{-2} from low-temperature specific heat data [15]. In the range of low Os concentrations, the decrease of γ and the increase of the Néel temperature T_N with increasing Os concentration are consistent with the spin fluctuation theory proposed by Hasegawa [25]. According to his SCR calculations for the specific heat of weakly antiferromagnetic materials, there is a linear relationship between the γ value and $T_N^{3/4}$. The validity of the theory has been confirmed by data on β-MnFe, -MnCo and -MnNi alloys [15], in which the substitutional atoms preferentially occupy site 1 in analogy with β-MnOs alloys. Therefore, it could be concluded that the β-MnOs alloys in the range of low Os concentration are itinerant-type weak antiferro-

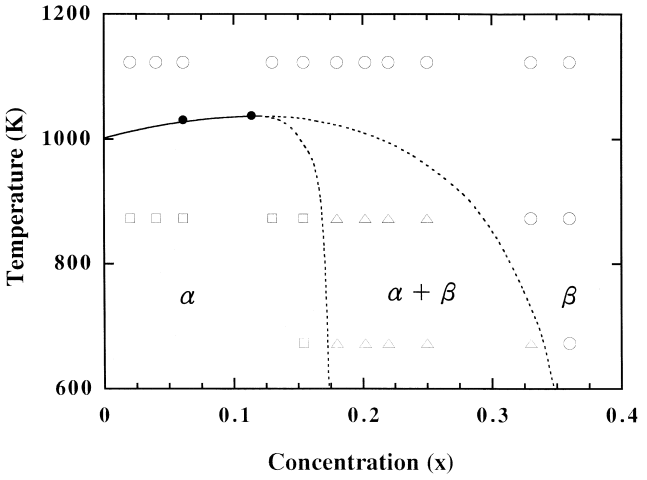

Fig. 5. Phase diagram of the Mn–Os system. The open symbols are for the data obtained by X-ray diffraction: (○) β-phase, (△) mixed phase (α+β), (□) α-phase. (●) Phase transition temperature determined from DSC measurements.

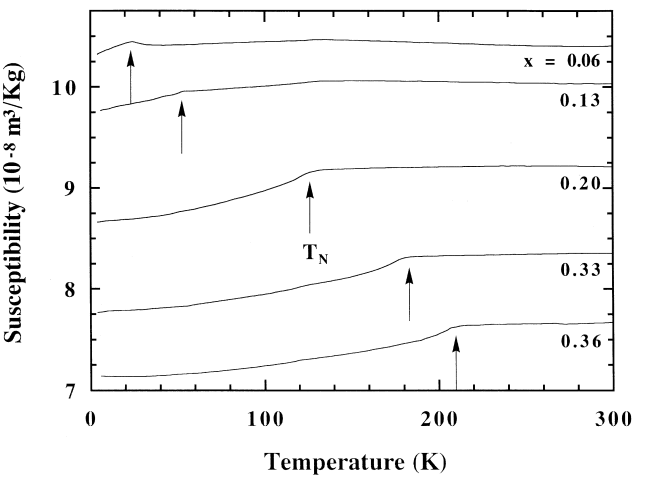

Fig. 6. Temperature dependence of the magnetic susceptibility of β-$Mn_{1-x}Os_x$ ($x = 0.06$, 0.13, 0.20, 0.33 and 0.36) alloys. The arrows indicate the Néel temperature, T_N.

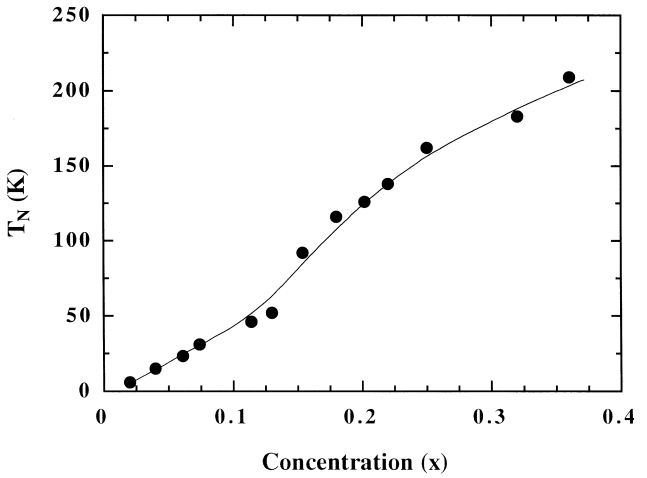

Fig. 7. Concentration dependence of the Néel temperature T_N of β-$Mn_{1-x}Os_x$ alloys.

magnets and the significantly large value of γ is closely correlated with the spin fluctuations.

4. Conclusion

The X-ray powder diffraction measurements of $Mn_{1-x}Os_x$ ($x \leqq 0.36$) alloys were carried out in order to investigate the existence of the α, β and γ phases and the concentration dependence of the lattice constant of β-$Mn_{1-x}Os_x$ alloys. Moreover, measurements of the temperature dependence of the magnetic susceptibility and the specific heat of β-Mn alloys were performed. The main results are summarized as follows.

1. Using X-ray powder diffraction and DSC data, the phase diagram up to $x = 0.36$ was established for the first time.

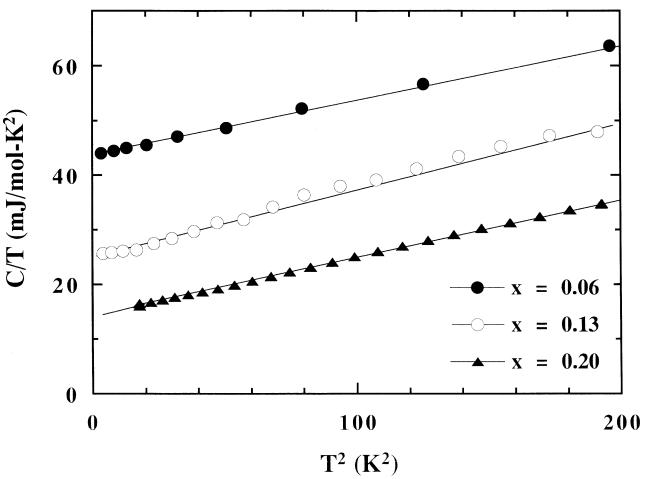

Fig. 8. Temperature dependence of the low-temperature specific heat in the form of C/T–T^2 plots for β-$Mn_{1-x}Os_x$ ($x = 0.06$, 0.13 and 0.20) alloys.

2. In samples ($x \leqq 0.36$) quenched from 1123 K, the β-Mn phase in which Os atoms preferentially occupy site 1 is stabilized.
3. The room temperature lattice constant and the Néel temperature of β-$Mn_{1-x}Os_x$ alloys increase with increasing Os concentration.
4. The electronic specific heat coefficient γ of β-$Mn_{1-x}Os_x$ alloys is large and decreases gradually with increasing Os concentration. Such a large γ value could be correlated with spin fluctuations.

Acknowledgements

The authors wish to express their thanks to Mr. H. Tanaka for experimental support in the present study. One of the authors (R.Y) was supported by a Research Fellowship of the Japan Society for the Promotion of Science for Young Scientists.

References

[1] C.G. Shull, M.K. Wilkinson, Rev. Mod. Phys. 25 (1953) 100.
[2] J.S. Kasper, B.W. Roberts, Phys. Rev. 101 (1956) 537.
[3] T. Yamada, N. Kunitomi, Y. Nakai, D.E. Cox, G. Shirane, J. Phys. Soc. Jpn. 28 (1970) 615.
[4] Y. Endoh, Y. Ishikawa, T. Shinjo, Phys. Lett. 29A (1969) 310.
[5] T.J. Hicks, A.R. Pepper, J.H. Smith, J. Phys. C 1 (1968) 1683.
[6] E. Krén, Phys. Lett. 21 (1966) 383.
[7] B. Dieny, V.S. Speriosu, S.S.P. Parkin, B.A. Gurney, D.R. Wilhoit, D. Mauri, Phys. Rev. B 43 (1991) 1297.
[8] M. Tsunoda, Y. Tsuchiya, M. Kotono, M. Takahashi, J. Magn. Magn. Mater. 171 (1997) 29.
[9] H.N. Fuke, K. Saito, Y. Kamiguchi, H. Iwasaki, M. Sahashi, J. Appl. Phys. 81 (1997) 4004.
[10] R. Yamauchi, K. Fukamichi, H. Yamauchi, A. Sakuma, J. Alloys Comp. 279 (1998) 93.
[11] A. Sakuma, J. Phys. Soc. Jpn. 68 (1999) 620.
[12] R. Yamauchi, K. Fukamichi, H. Yamauchi, A. Sakuma, J. Echigoya, J. Appl. Phys. 85 (1999) 4741.
[13] T. Yamaoka, J. Phys. Soc. Jpn. 36 (1974) 445.
[14] R. Kohlhaas, W.D. Weiss, Z. Naturforsch. 24a (1969) 287.
[15] T. Shinkoda, K. Kumagai, K. Asayama, J. Phys. Soc. Jpn. 46 (1979) 1754.
[16] M. Katayama, S. Akimoto, K. Asayama, J. Phys. Soc. Jpn. 42 (1977) 97.
[17] T. Kohara, K. Asayama, J. Phys. Soc. Jpn. 37 (1974) 37.
[18] H. Nakamura, M. Shiga, Physica B 237/238 (1997) 453.
[19] H. Nakamura, K. Yoshimura, M. Shiga, M. Nishi, K. Kakurai, J. Phys. Condensed Matter 9 (1997) 4701.
[20] M. Mekata, Y. Nakanishi, Y. Yamaoka, J. Phys. Soc. Jpn. 37 (1974) 1509.
[21] T. Hori, J. Phys. Soc. Jpn. 38 (1975) 1780.
[22] S. Akimoto, T. Kohara, K. Asayama, Solid State Commun. 16 (1975) 1227.
[23] Y. Nishihara, S. Ogawa, S. Waki, J. Phys. Soc. Jpn. 42 (1977) 845.
[24] M. Katayama, K. Asayama, J. Phys. Soc. Jpn. 44 (1978) 425.
[25] H. Hasegawa, J. Phys. Soc. Jpn. 38 (1975) 1780.
[26] W. Williams Jr., J.L. Stanford, J. Magn. Magn. Mater. 1 (1976) 271.
[27] K. Sasao, R. Yamauchi, K. Fukamichi, H. Yamauchi, IEEE Trans. Magn. 35 (1999) 3910.

[28] D.A. Young, Phase Diagrams of the Elements, University of California Press, Berkeley, CA, 1991.
[29] V.E. Raub, W. Mahler, Z. Metallkd. 46 (1955) 282.
[30] K. Adachi, J. Phys. Soc. Jpn. 35 (1973) 426.
[31] M. Shiga, H. Nakamura, M. Nishi, K. Kakurai, J. Magn. Magn. Mater. 140–144 (1995) 2009.
[32] J.R. Stewart, R. Cywinski, Phys. Rev. B 59 (1999) 4305.
[33] M. Matsui, K. Sato, K. Adachi, J. Phys. Soc. Jpn. 35 (1973) 419.
[34] Y. Kohori, Y. Noguchi, T. Kohara, J. Phys. Soc. Jpn. 62 (1993) 447.
[35] N. Mori, T. Ukai, K. Sasaki, in: P. Rhodes (Ed.), Physics of Transition Metals, Institute of Physics Conference Series, Vol. 55, Bristol Institute of Physics, 1980, p. 21.